Assessing stacking faults in Bi–Sr–Ca–Cu–O phases by X-ray diffraction

R. MANAILA, L. MIU
Institute of Physics and Technology of Materials, Bucharest, P.O.B. MG7, Romania
M. ZAHARESCU
Research Center for Physical Chemistry, Splaial Independentei 202A, Bucharest, Romania

A Hendricks–Teller analysis of the X-ray diffraction line shifts in Bi–Sr–Ca–Cu–O phases allows an estimate of the stacking fault probabilities (missing or extra Cu–O layers). The probability values suggest some conclusions about the mutual relationships of the 2201, 2212 and 2223 phases and the kinetics of their formation.

1. Introduction

Stacking faults are currently reported in samples prepared in the Bi–Sr–Ca–Cu–O and related systems. In a somewhat restricted sense of the term, they signify the occurrence of the wrong number of Cu–O planes in the elementary cell of a $Bi_2Sr_2Ca_{n-1}Cu_nO_x$ phase (2201, 2212 or 2223 for $n = 1$, 2 and 3, respectively). This accounts for the occasional finding of 1 or 3 Cu–O layers in a half-cell of the 2212 phase (correct number: 2) or 2 Cu–O layers in a half-cell of the 2223 phase (correct number: 3). The presence of stacking faults appears natural if we consider the mutual relationship (polytypism) between the 2201, 2212 and 2223 phases. The main difference between them is the number of Cu–O layers per unit cell (thickness of the perovskite block), which determines the length of the c axis ($c \simeq 2.4$ nm, 3.06 nm and 3.71 nm for $n = 1, 2$, and 3, respectively). We should mention here that, although the formula for the $n = 1$ phase is usually written as $Bi_2Sr_2CuO_x$, investigation of the first synthesis stages of this phase [1] revealed that Ca is the first to enter it.

The number of Cu–O layers per elementary cell seems to be related to the superconducting critical temperature (T_c) of the phase [2]. The continuous increase of T_c with the number of Cu–O layers in both Bi-Based and Tl-based systems strongly suggests that such a relationship exists. In the Tl–Ba–Ca–Cu–O system, it was reported [3] that the presence of intergrowths of the 2212 phase inside 2223 crystals reduces T_c by ~ 7 K, in comparison with defect-free crystals. This could explain the range of T_c values reported from resistivity and Meissner data for double and triple CuO_2 layer structures in this system. Therefore, the presence of stacking faults (SF) is also likely to alter the critical temperature.

On the other hand, estimating the frequency of SF, e.g. in the 2212 samples obtained by different procedures, could shed some light on the kinetics of obtaining the 2223 phase from the 2212 one. Experimental evidence suggests that the 2223 phase appears by inserting an additional Cu–O + Ca–O pair of layers (per half-cell) into the stable 2212 phase. The kinetics of this process seems to be very sluggish, requiring long annealing time close to the melting temperature, in order to facilitate ion migration. Different procedures were found, which reportedly accelerate this process, e.g. partial substitution of Bi by Pb [4, 5], Bi and Cu excess over the 2212 composition [6], vacuum precalcination [7].

Stacking faults were noticed in the 2223 phase [8] in a TEM lattice image taken with the electron beam normal to the c axis, along which the Bi–Bi interlayer distance is normally ~ 1.9 nm. However, every 5 to 10 layers, a 1.5 nm spacing is observed, indicative of the presence of two Cu–O layers instead of three. Also, high-resolution imaging of a 3.7 nm phase grain [9] showed coherent intergrowth of lamellae of the 3.0 nm phase, comprising up to three smaller Bi–Bi distances. Moreover, lamellae with a width larger than 1.85 nm were noticed, maybe similar to the 4 Cu–O layers phase (1234) in the Tl–Ba–Ca–Cu–O system [10].

Lattice images reported by Veblen *et al.* [11] for the 3.0 nm phase show defects consisting of a missing or an extra perovskite unit of ~ 0.4 nm thickness, normal to the c axis. Also, Ramesh *et al.* [12] found by HREM* and convergent beam electron diffraction that, at some spots inside a 3.0 nm grain, three Cu–O layers are present instead of two, as can be seen from the spacing difference of the Bi layers. Energy dispersive spectroscopy (EDXS) confirmed that the regions with a higher concentration of such faults also have a higher Ca and Cu concentration [12]. Stacking faults and larger scale intergrowths are also frequently reported in the related system Tl–Ba–Ca–Cu–O, as revealed by transition electron microscopy (TEM) studies ([13] and the papers quoted therein).

X-ray diffraction is sensitive to the presence of SF (extra or missing perovskite blocks) which cause predictable changes in the position and width of the diffraction lines. This prompted us to write a computer program which uses the position of diffraction

* High resolution electron microscopy

0022–2461/91 $03.00 + .12

lines, in order to derive best-fit values for the SF probability and for the c axis length in 2201, 2212 and 2223 phases.

2. Hendricks–Teller analysis of SF effect

In a paper [14], Hendricks and Teller (H–T) calculated the diffraction pattern for layer lattices in which different types of disorder are introduced, concerning the scattering power of the layers and/or the mutual phase shifts between neighbouring layers. Thus, the problem of n types of layers, each having a φ_n contribution to the mutual phase shift, can be tackled.

The structure of the three main phases in the Bi–Sr–Ca–Cu–O system can be envisaged as a stacking of $Bi_2Sr_2O_4$ sandwiches [8] which make the main contribution to the scattered intensity. The Cu–O + Ca–O layers which separate these sandwiches scatter much less but their number essentially determines the distance between the Bi–Sr–O layers. Thus, the problem can be reduced to that of a single type of complex layer (Bi–Sr–O) but the phase shift φ between successive layers can take three series of values φ_i, corresponding to the distances $d_i = c_i/2$ between the Bi–Sr–O planes in the three phases (c = crystallographic axis normal to the layers): phase 2201: $c_1/2 \simeq 1.2$ nm $= d_1$; phase 2212: $c_2/2 \simeq 1.5$ nm $= d_2$; phase 2223: $c_3/2 \simeq 1.85$ nm $= d_3$. And $\varphi_i = kd_i$, where $k = (4\pi/\lambda)\sin\theta$ is the scattering vector and θ is the Bragg angle.

In the general formalism of H–T, the diffracted intensity

$$I = |F|^2(1-C^2)/(1-2C\cos\bar{\varphi} + C^2) \quad (1)$$

where $C = \langle\cos(\varphi - \bar{\varphi})\rangle$ and the average $\bar{\varphi}$ is defined by

$$\langle\sin(\varphi - \bar{\varphi})\rangle = 0. \quad (2)$$

Here, F is the structure factor for the $Bi_2Sr_2O_4$ layer and the average, $\langle\ \rangle$, is taken over the volume investigated.

Let us restrict ourselves to the case of interest, where only two φ_i are present: the dominant one, φ_o, correct for the phase being investigated and φ_{SF}, corresponding to a particular type of SF within this phase. Then, if P is the probability of the SF appearing

$$\begin{aligned} I = {} & |F|^2[1 - P^2 - (1-P)^2 \\ & - 2P(1-P)\cos(\varphi_{SF} - \varphi_o)]/[1 + P^2 \\ & + (1-P)^2 + 2P(1-P)\cos[\varphi_{SF} - \varphi_o) \\ & - 2(1-P)(\cos\varphi_{SF} + \cos\varphi_o)] \\ = {} & |F|^2\,\mathrm{Num/D} \end{aligned} \quad (3)$$

if we take into account the definition in Equation 2.

In the vicinity of a diffraction peak of the main phase:

$$\varphi \simeq n2\pi + \delta;\ \cos\varphi \simeq 1 - \delta^2/2$$
$$\text{with } n = \text{integer}$$

and the denominator, D, which determines the position of the peak, can be written as [8]

$$D \simeq a\varphi^2 + b\varphi + c \quad (4)$$

where $a = 1 - P - P(1-P)\cos\varphi_{SF}$; $b = 2P(1-P)\sin\varphi_{SF}$, $c = 2P^2(1-\cos\varphi_{SF})$.

Thus, $I(k)$ can be described by a Lorentzian

$$\begin{aligned} I & \sim |F|^2\,\mathrm{Num}/(a\varphi^2 + b\varphi + c) \\ & = |F|^2\,\mathrm{Num}/[1 + k^2(\varphi - \varphi_d)^2] \end{aligned} \quad (5)$$

with $\varphi_d = -b/2a$ determining the shift of the peak, due to the stacking fault probability, P. The argument above applies to $(00l)$ lines only, which are determined by the interlayer interferences.

3. The optimization program

The program works by minimizing the relative difference between the calculated and observed diffraction angles 2θ. For this purpose, three parameters are varied: the SF probability, P; the c axis value; and a θ-independent instrumental shift Y, which could be caused by sample surface displacement out of the diffractometer axis.

Only the $(00l)$ lines participate in the optimization of P, while all the lines are taken into account for the refinement of c and Y. The residue

$$R = \left\{\sum_{1i}^{N}[(2\theta_{calc})_i - (2\theta_{exp})_i]^2/(N-1)\right\}^{1/2} \quad (6)$$

was calculated for the N diffraction lines, where $2\theta_{calc} = 2\arcsin(\lambda/2d) + \mathrm{DEP} + \mathrm{Y}$ and $d = 1/[(h^2 + k^2)/a^2 + l^2/c^2]^{1/2}$,

with $a = 0.53909$ nm (an average value for the pseudo-tetragonal lattice) and λ is the radiation wavelength.

The line shift DEP, caused by the stacking faults was approximated, after Equations 4 and 5 as

$$\begin{aligned} \mathrm{DEP} = {} & -180\lambda P(1-P)\sin(kc_{SF}/2)/\pi^2 c\cos\theta \\ & \times[1 - P - P(1-P)\cos(kc_{SF}/2)], \end{aligned} \quad (7)$$

where c and c_{SF} correspond to the majority phase and the SF one, respectively. Equation 7 yields DEP in °2θ. This shift applies to the $(00l)$ lines only.

The presence of stacking faults causes an additional line broadening as well, which also is roughly proportional to P. However, we relied in the present work on the line shifts only.

The parameters, c and Y, were assigned starting values, close to the expected ones, while P was initialized to 0. Each parameter was varied in turn, by a fixed increment. The first parameter was varied, while the other two were maintained constant, until the residue reached a minimum. The value corresponding to this minimum was assigned to the mobile parameter and the second parameter started its variation, the first and third ones being kept fixed. When all three parameters were optimized, a new cycle started with the optimized values for the second and third parameters, while the first one was initialized at its starting value.

The residue, R (r.m.s. deviation), was found to decrease steadily inside each cycle as well as between cycles until an absolute minimum, R_o, was reached, typically after 3 to 20 cycles. The R_o value can be taken as defining the quality of the fit. Values ranging between 0.003 and 0.12 were found for R_o in most of the runs.

The order in which the three parameters were optimized was found to bring no or only minor changes in the final values and residue. For each sample and each phase (each set of diffraction lines), two optimization runs were taken, in the following conditions: (a) Y, P and c are free to vary until reaching a minimal residue; and (b) Y is kept constant at a value determined by calibration of line positions with an internal KCl standard, while P and c are free to vary.

4. Results and discussion

The program was used to process diffraction data taken with CuK_α radiation on two series of samples in the system Bi–Sr–Ca–Cu–O, with prepared composition 4–3–3–4 (series M) and 4–2.6–2.6–4 (series L). Also, a 2–2–2–3 sample with Pb addition [15] was investigated. The samples were prepared by solid state reaction at different temperatures and submitted to different annealing procedures (see Table I). The program was also applied to the 2–2–2–3 sample reported by Tarascon *et al.* [8], using the data read from Fig. 4 in their paper. This sample is denoted by T in the following.

The samples comprised one or several phases from the series $Bi_2Sr_2Ca_{n-1}Cu_nO_x$ with $n = 1$ (phase 1, 2201, $c_1 \simeq 2.4$ nm), $n = 2$ (phase 2, 2212, $c_2 \simeq 3.0$ nm) and $n = 3$ (phase 3, 2223, $c_3 \simeq 3.7$ nm) (Table I). Additional phases (unreacted CuO and carbonates, mixed Bi–Cu–Ca–Sr oxides) were found only occasionally in the samples calcined above 800 °C.

In phase 2 we tried to determine both P_1 (the probability of finding 1 Cu–O layer) and P_3 (the probability of finding three Cu–O layers per half-cell, instead of the correct value of two). In phase 1 we looked for P_2 and, in phase 3, P_2 was searched for too.

A number of 3 to 13 diffraction lines was generally used in the optimization, depending on the concentration of the phase in the sample being investigated, i.e. depending on the general level of line intensities. Partially overlapped lines were avoided, as were also higher angle ones, where several reflections are usually superimposed. Taking into account these poorly indexable lines was found generally to increase the final residue.

Table I shows the optimized c parameter and stacking fault probabilities P_1, P_2 and P_3 in different samples and different phases. The values given are those corresponding to the run with minimal final residue. Exception was made for sample T, where the P_2 value corresponds to the instrumental shift Y and to the c_3 axis being fixed at the values 0 and 3.708 nm respectively (as reported in [8]). For obtaining P_3 in sample T, only Y was kept constant at 0. It ought to be mentioned that the P_2 value found in this sample ($P_2 = 0.26$), on the basis of the (0010), (0012) and (0014) lines, closely agrees with that reported in [8] (where $P_2 = 0.25$).

Fig. 1a and b displays the P_i and c_i values ($i = 1, 2, 3$) for a selection of samples. The error bar encompasses the results obtained from all optimization runs, performed for a given set of diffraction lines, under different assumptions.

Several observations can be made on the data in Table I and Fig. 1.

The SF probability P_3 in the 2212 phase is vanishing in preparations which contain phases 2 and 1 only. However, P_3 reaches measurable values in some of the cases when the 2223 phase is also present in considerable amounts (samples L2 and especially T). In both these latter samples, the 2223 phase also shows a considerable P_2 value (Fig. 1a).

Samples L2 and T are examples of 2223 phases which are still poorly separated from the precursor

TABLE I Stacking fault probabilities P and c axis values, as obtained by the optimization procedure. P_i = probability of finding i Cu–O layers in a half-cell.

Sample	Composition prepared	Annealing	Phases	Phase 1 (2201)		Phase 2 (2212)			Phase 3 (2223)	
				P_2	c_1 (nm)	P_3	P_1	c_2 (nm)	P_2	c_3 (nm)
L_1	4–2.6–2.6–4	5 ON[a] at increasing T between 790–845 °C	2 + (1)[b]			0	0.03	3.055		
L_2	"	as L_1, additional 4 days at 868 ± 3 °C partially melted	3 + 2 + 1			0.04	0	3.060	0.34	3.694
L_3	"	as L_1, additional 1 day at 868 °C	1 + (2)			0	0.03	3.064		
M_1	4–3–3–4	4 h at 730 °C	1	0.07	2.451					
M_2	"	4 h at 770 °C	1 + ((2))	0	2.461					
M_3	"	24 h at 800 °C	2 + ((1))			0	0.08	3.062		
M_4	"	24 h at 850 °C	2 + ((1))			0	0.06	3.058		
G	2–2–2–3 + Pb	1 ON at 800 °C + 500 h at 845 °C	2 + 3			0.01	0	3.077	0	3.704
T	2–2–2–3	[8]	3 + (2)			0.08[c]	[c]	3.073[c]	0.26	3.708[d]

[a] ON = overnight ≃ 17 h; 1 day = 24 h; [b] ( ) = small amounts; (( )) = traces; [c] low precision data (very broad lines); [d] parameter fixed during optimization.

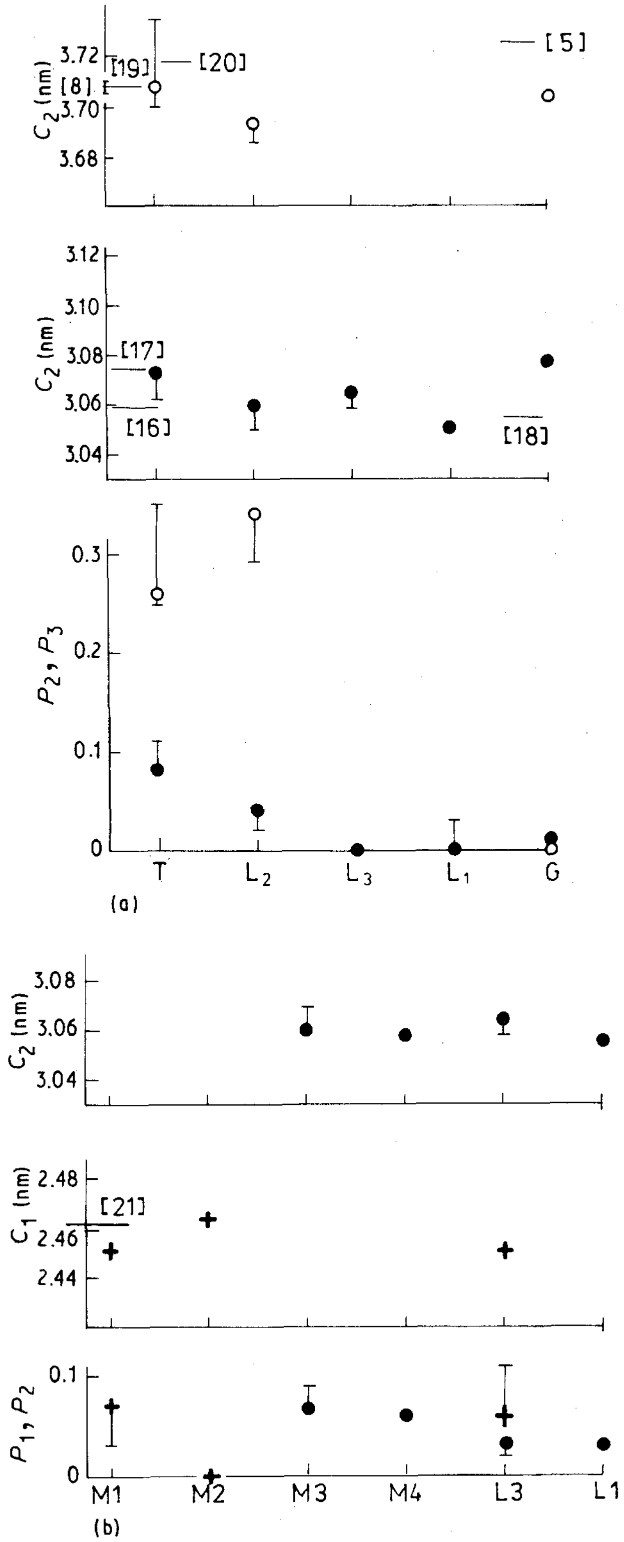

Figure 1 Stacking fault probabilities P and c axis values for selected samples: (a) • P_3 for phase 2, ○ P_2 for phase 3; (b) • P_1 for phase 2, + P_2 for phase 1. Points indicate the results with minimal residue. Error bars give the maximum deviation between data obtained in optimization variants. Data from references are marked with [ ].

2212 phase and contain frequent SFs of the latter type. The 2212 phase also contains "germs" of the 2223 phase, as SFs of the latter type.

On the contrary, sample G displays a well-ordered stacking for the 2212 and 2223 phases (Fig. 1a), P_3 and P_2 both being close to 0. In this sample, the two phases are clearly separated. Thus, sample G seems to represent the final stage of 2223 segregation from its 2212 precursor, while samples L2 and T are intermediate stages.

The data in Fig. 1a are illustrated by the diffraction patterns in Fig. 2a and b. It can be seen that lines of the 2223 phases which are strongly faulted (L2 and T) display shifts from the calculated positions towards neighbouring 2212 lines and also are considerably broadened. On the contrary, in sample G both the (0010) and (0014) lines of this phase are relatively narrow and located close to the calculated positions. The same observations can be made concerning the lines of the 2212 phase in these samples (Fig. 2).

Phase 2212 shows, in most L and M samples, small (< 0.1) probabilities P_1 of finding a single Cu–O layer instead of two (Table I, Fig. 1b), pointing to a rather good separation of this phase from the 2201 precursor, even in the first formation stages (around 800 °C). Also, phase 1 is found to possess only slightly faulted stackings ($P_2 < 0.1$) irrespective of the annealing temperature.

These observations suggest that the formation of the 2212 phase from the 2201 one is relatively easy. Germs (stacking faults) of 2212 inside 2201 readily grow into fully-developed crystallites of the former phase, with low P_1 values. On the contrary, the 2223 phase which appears inside 2212 is strongly faulted in its first formation stages.

The c values for the 2201, 2212 and 2223 phases, as determined by the optimization program, are also shown in Table I and Fig. 1. For the 2212 phase, they are in the range of values reported in the literature for Sr/Ca = 1 ratio [16, 17]. The c_2 axis of the 2212 phase is expected to increase when 2223-type faults are present, while that of the 2223 phase (c_3) should decrease upon faulting. A slight tendency in this sense can be noticed in Fig. 1a. However, a corresponding trend, relating phases 2201 and 2212, is absent in Fig. 1b.

5. Conclusions

The analysis of stacking fault probabilities in a series of samples, prepared in different conditions, confirms a strong structural relationship between the 2201, 2212 and 2223 phases in the Bi–Sr–Ca–Cu–O system. These phases seem to form each from the preceding one, by insertion of additional Cu–O and Ca–O layers, when the temperature and/or annealing time are increased or, generally, when ion migration is enhanced. In this process, imperfect stacking (memory of the precursor stacking) could be characteristic for a given phase in the first stages of its formation, while further annealing can lead to stacking improvement. Stacking defects of the "next" phase-type could also be seen as nuclei for growing this phase inside the dominant one.

The stacking defects could influence the mechanical properties of the material, which are essential for its applications. Also these faults, inside a grain of superconducting phase, could act as pinning centres for the magnetic flux lines. Work is now in progress to search for a correlation between SF probabilities and

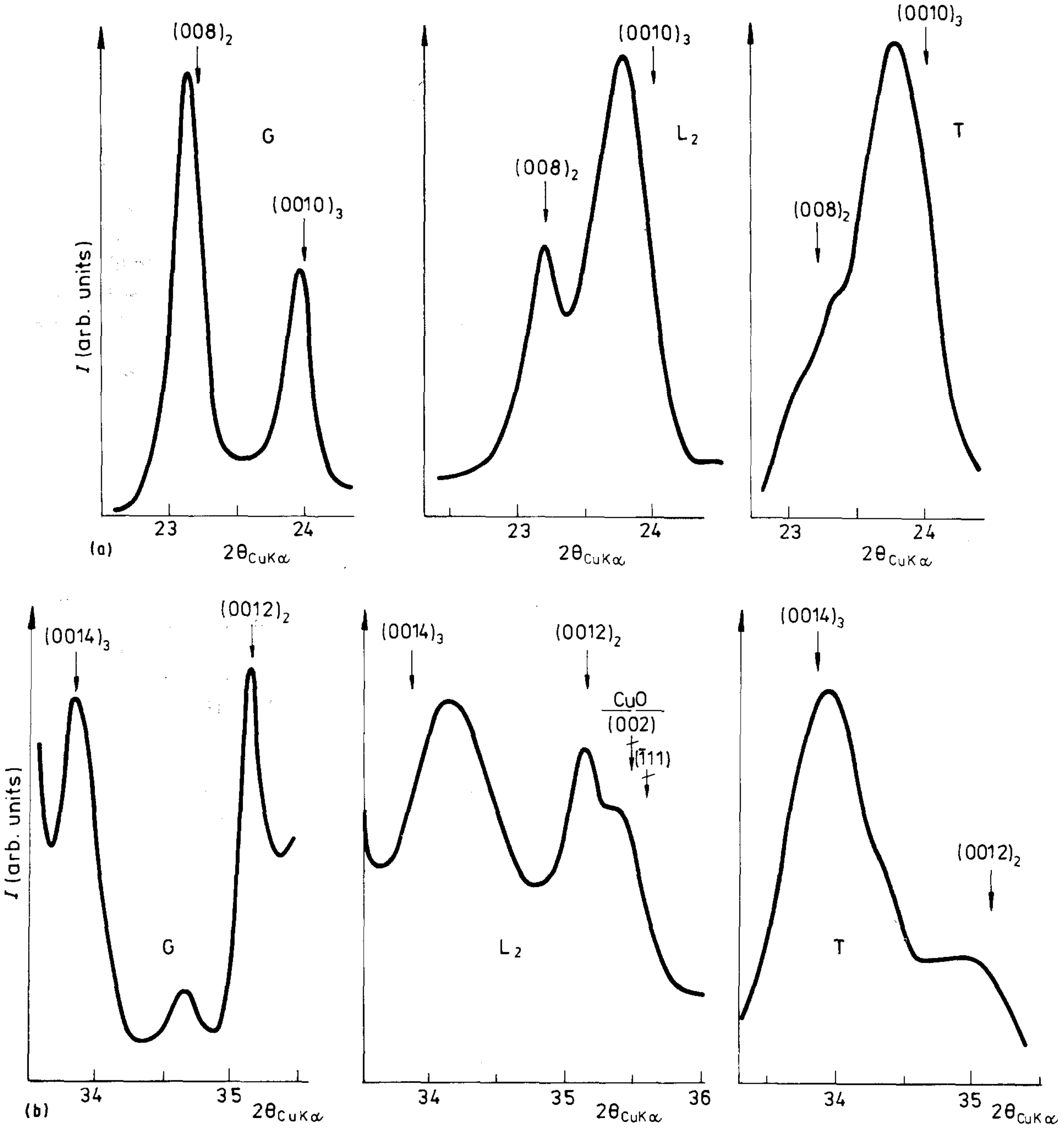

Figure 2 Fragments of the diffraction patterns for selected samples. Ideal positions for 2223 and 2212 lines were calculated with $c_3 = 3.708$ nm and $c_2 = 3.064$ nm, respectively. X = unidentified line. The phase to which each line belongs is marked as subscript.

inductively measured T_c in samples of the Bi–Sr–Ca–Cu–O system.

Acknowledgements

Our thanks are due to Dr G. Aldica for supplying the G sample. We also gratefully acknowledge the kind assistance of the Humboldt Foundation (FRG), which provided us an IBM PS 2 computer.

References

1. M. ZAHARESCU and R. MANAILA, in press.
2. J. M. WHEATLEY, T. C. HSU and P. W. ANDERSON, *Nature* **333** (1988) 121; S. S. P. PARKIN, E. M. ENGLER, V. Y. LEE, A. I. NAZZAL, Y. TOKURA, J. B. TORRANCE and P. M. GRANT, Unpublished work (quoted in [12]).
3. S. S. P. PARKIN, V. Y. LEE, E. M. ENGLER, A. I. NAZZAL, T. C. HUANG, G. GORMAN, R. SAVOY and R. BEYERS, *Phys. Rev. Lett.* **60** (1988) 2539.
4. E. CHAVIRA, R. ESCUDERO, D. RIOS-JARA and L. M. LEÓN, *Phys. Rev. B* **38** (1988) 9272.
5. M. TAKANO, J. TAKADA, K. ODA, H. KITAGUCHI, Y. MIURA, Y. IKEDA, Y. TOMII and H. MAZAKI, *Jap. J. Appl. Phys.* **27** (1988) L 1041.
6. T. WADA, N. SUZUKI, A. MAEDA, S. UCHIDA, K. UCHINOKURA and S. TANAKA, *ibid.* **27** (1988) 430.
7. N. UNO, N. ENOMOTO, Y. TANAKA and H. TAKAMI, *Ibid.* **27** (1988) L 1013.
8. J. M. TARASCON, W. R. McKINNON, P. BARBOUX, D. M. HWANG, B. G. BAGLEY, L. H. GREENE, G. W. HULL, Y. LePAGE, N. S. STOFFEL and M. G. GIROUD, *Phys. Rev. B* **38** (1988) 8885.
9. G. Van TENDELOO, H. W. ZANDBERGEN, J. Van LANDUYT and S. AMELINCKX, *Appl. Phys. A* **46** (1988) 153.
10. H. IHARA, R. SUGISE, M. HIRABAYASHI, N. TERADA, M. JO, K. HAYASHI, A. NEGISHI, M. TOKUMOTO, Y. KIMURA and T. SHIMOMURA, *Nature* **334** (1988) 510.

11. D. R. VEBLEN, P. J. HEANEY, R. J. ANGEL, L. W. FINGER, R. M. HAZEN, C. T. PREWITT, N. L. ROSS, C. W. CHU, P. H. HOR and R. L. MENG, *ibid.* **332** (1988) 334.
12. J. R. RAMESH, C. J. D. HETHERINGTON, G. THOMAS, S. M. GREEN, C. JIANG, M. L. RUDEE and H. L. LUO, *Appl. Phys. Lett.* **53** (1988) 615.
13. R. B. BEYERS, S. S. P. PARKIN, V. Y. LEE, A. I. NAZZAL, R. J. SAVOY, G. L. GORMAN, T. C. HUANG and S. J. LaPLACA, *IBM J. Res. Develop.* **33** (1989) 228.
14. S. HENDRICKS and E. TELLER, *J. Chem. Phys.* **10** (1942) 147.
15. L. MIU, GH. ALDICA, E. CRUCEANU and V. TEODORESCU, *J. Mater. Sci. Lett.* **9** (1990) 532.
16. G. S. GRADER, E. M. GYORGY, P. K. GALLAGHER, H. M. O'BRYAN, D. W. JOHNSON, Jr, S. SUNSHINE, S. M. ZAHURAK, S. JIN and R. C. SHERWOOD, *Phys. Rev. B* **38** (1988) 757.
17. M. YOSHIDA, *Jap. J. Appl. Phys.* **27** (1988) L 2044.
18. Y. YAMADA and S. MURASE, *ibid.* **27** (1988) L 996.
19. Y. IKEDA and M. TAKANO, *ibid.* **27** (1988) L 2067.
20. U. ENDO and S. KOYAMA, *ibid.* **27** (1988) L 1476.
21. C. C. TORARDI, M. A. SUBRAMANIAN, J. C. CALABRESE, J. GOPALAKRISHNAN, E. M. McCARRON, K. J. MORRISSEY, T. R. ASKEW, R. B. FLIPPEN, U. CHOWDRY and A. W. SLEIGHT, *Phys. Rev. Lett.* **38** (1988) 225.

Received 20 February and accepted 3 December 1990